Performance of the Imaging Atmospheric Cherenkov Telescope System of CANGAROO-III

T. Yoshikoshi[a], Y. Adachi[a], A. Asahara[b], G.V. Bicknell[c], R.W. Clay[d], Y. Doi[e],
P.G. Edwards[f], R. Enomoto[a], S. Gunji[e], S. Hara[a], T. Hara[g], T. Hattori[h], Sei. Hayashi[i],
Y. Higashi[b], R. Inoue[h], C. Itoh[j], S. Kabuki[b], F. Kajino[i], H. Katagiri[b], A. Kawachi[h],
S. Kawasaki[a], T. Kifune[k], R. Kiuchi[a], K. Konno[e], L.T. Ksenofontov[a], H. Kubo[b],
J. Kushida[h], Y. Matsubara[l], Y. Mizumoto[m], M. Mori[a], H. Muraishi[n], Y. Muraki[l], T. Naito[g],
T. Nakamori[b], D. Nishida[b], K. Nishijima[h], M. Ohishi[a], J.R. Patterson[d], R.J. Protheroe[d],
Y. Sakamoto[h], M. Sato[e], S. Suzuki[o], T. Suzuki[o], D.L. Swaby[d], T. Tanimori[b], T. Tanimura[b],
G.J. Thornton[d], K. Tsuchiya[a], S. Watanabe[b], T. Yamaoka[i], M. Yamazaki[i], S. Yanagita[o],
T. Yoshida[o], M. Yuasa[a] and Y. Yukawa[a]
(a) Institute for Cosmic Ray Research, University of Tokyo, Kashiwa, Chiba 277-8582, Japan
(b) Department of Physics, Graduate School of Science, Kyoto University, Sakyo-ku, Kyoto 606-8502, Japan
(c) Research School of Astronomy and Astrophysics, Australian National University, ACT 2611, Australia
(d) Department of Physics and Mathematical Physics, University of Adelaide, SA 5005, Australia
(e) Department of Physics, Yamagata University, Yamagata, Yamagata 990-8560, Japan
(f) Institute of Space and Astronautical Science, Sagamihara, Kanagawa 229-8510, Japan
(g) Faculty of Management Information, Yamanashi Gakuin University, Kofu, Yamanashi 400-8575, Japan
(h) Department of Physics, Tokai University, Hiratsuka, Kanagawa 259-1292, Japan
(i) Department of Physics, Konan University, Kobe, Hyogo 658-8501, Japan
(j) Ibaraki Prefectural University of Health Sciences, Ami, Ibaraki 300-0394, Japan
(k) Faculty of Engineering, Shinshu University, Nagano, Nagano 480-8553, Japan
(l) Solar-Terrestrial Environment Laboratory, Nagoya University, Nagoya, Aichi 464-8602, Japan
(m) National Astronomical Observatory of Japan, Mitaka, Tokyo 181-8588, Japan
(n) School of Allied Health Sciences, Kitasato University, Sagamihara, Kanagawa 228-8555, Japan
(o) Faculty of Science, Ibaraki University, Mito, Ibaraki 310-8512, Japan
Presenter: T. Yoshikoshi (tyoshiko@icrr.u-tokyo.ac.jp), jap-yoshikoshi-T-abs1-og27-poster

The imaging atmospheric Cherenkov telescope system of CANGAROO-III has been in full operation with four 10 meter diameter telescopes since March 2004 near Woomera, South Australia. The system is used to study gamma-ray astrophysics at sub-TeV energies in the southern hemisphere. The performance of the stereoscopic system such as angular and energy resolutions for gamma rays has been investigated using Monte Carlo simulations, which are based on various calibration results, e.g., calibration of light collection efficiency using muon ring images. We present the estimated performance of the CANGAROO-III system as well as the reliability of our simulation code, comparing simulation results with observed data.

1. Introduction

The atmospheric Cherenkov technique has dramatically improved the signal-to-noise ratio in detecting Very High Energy (VHE, $\sim$ TeV) gamma rays by utilizing the imaging technique, which was first demonstrated by the Whipple 10 meter telescope in 1989 detecting gamma rays from the Crab Nebula at the 9 σ level [1]. Sensitivity to VHE gamma rays has further been improved by the HEGRA group by adding the technique of stereoscopic observations [2], in which two major backgrounds, local muon events and hadronic shower events, are greatly reduced owing to their locality (muons) and poor reconstruction accuracy due to more irregular

shower patterns (hadronic showers). Another important advantage of the stereoscopic system compared to a single Imaging Atmospheric Cherenkov Telescope (IACT) is its ability to reconstruct air shower parameters such as the arrival direction and the core location more accurately. As a result, we can expect to have better angular and energy resolutions using stereoscopic observations.

The CANGAROO team, which has played a pioneering role in the southern hemisphere, has been observing the southern sky since 1992, first with a 3.8 meter telescope equipped with a fine pixel camera (CANGAROO-I [3]) and, since March 2004, with a stereoscopic system (CANGAROO-III). Study of the total performance of the stereoscopic system is still underway and some preliminary results are presented here.

2. CANGAROO-III Stereoscopic IACT System

The CANGAROO-III stereoscopic IACT system is located near Woomera, South Australia. It consists of four 10 meter diameter IACTs, which are placed at the corners of a diamond shape with a 100 meter span. Data is acquired if any two telescopes are triggered within 650 ns [4] and raw trigger rates in this condition are about 20 Hz. The details of the optical system, the imaging cameras and the data acquisition system are described elsewhere [5, 6, 7]. The global (stereoscopic) trigger system has been in operation since December 2004 and the performance summarised here is for the previous two telescope system (T2 and T3) operated with the local trigger mode, in which the telescopes generate triggers individually. Most of the CANGAROO-III results reported at this conference are obtained with this older configuration.

3. Simulations

Our Monte Carlo simulation code consists of the following three parts: 1) primary particle injection and secondary particle generation in the atmosphere, 2) Cherenkov light emission from the particles and tracing it to the imaging cameras, and 3) response of the electronics. The air shower generation is based on GEANT3 [8] and the target atmosphere is approximated by uniform 80 layers of the same atmospheric depth, densities of which are calculated using the U.S. standard atmosphere. Only Rayleigh scattering is incorporated as a scattering process for Cherenkov photons in the atmosphere. Light collection efficiency of the telescope including electronics response is adjusted on the basis of the results from muon ring analysis, which is described in the following subsection. In the simulations used here, gamma rays of various energies are injected into the atmosphere inside of a circular area of the 500 meter radius at random.

3.1 Muon Ring Analysis

The data taken with the local trigger mode are used in the muon ring analysis. First, the hit pattern of each event is fitted to an arc. Then, relatively fine ring images satisfying the following conditions are selected: 1) number of hit pixels $\geq$ 15, 2) arc-lengths > 2° and 3) χ^2 normalized by the pixel size and divided
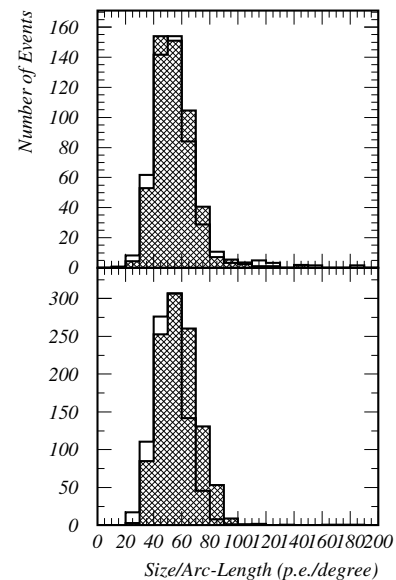

Figure 1. 'Size / arc-length' distributions for T2 (top) and T3 (bottom). The solid and hatched histograms are obtained from observed data and simulations, respectively.

by the number of hit pixels < 1.5. The curvature distribution of the selected events has a single peak around 0.75 deg.$^{-1}$ and purity of muon ring events is high enough in this calibration (note that the curvature is not used in the above event selection). The solid histograms in Figure 1 are distributions of 'size / arc-length' of the selected events. This amount is an indicator of the light collection efficiency of a telescope. The simulation code has been tuned with this result as well as with the results of optical measurements such as mirror reflectivity. The hatched histograms in Figure 1 are obtained using the simulation code and systematic uncertainty of the collection efficiency is at the 5% level.

4. Performance of the System in the Current Analyses

The angular and energy resolutions are estimated using the simulation code described above. We assume a point source at the center of the field of view with a power-law spectral index of -2.5. The simulated data is analyzed using the same procedures as for the SN 1006 data presented at this conference [9].

4.1 Angular Resolution

The arrival direction of a stereoscopic event is simply estimated as the intersection of major axes of individual Cherenkov images. Figure 2 shows distributions of reconstructed arrival directions in the field of view. X and Y projections of the distribution are well fitted by Lorentzians and here we define the angular resolution as FWHM obtained from the Lorentzian fit, which is $0°.294 \pm 0°.006$ for gamma rays vertically injected into the atmosphere. The resolution is almost constant up to the zenith angle of $20°$ and gradually gets worse at zenith angles greater than that.
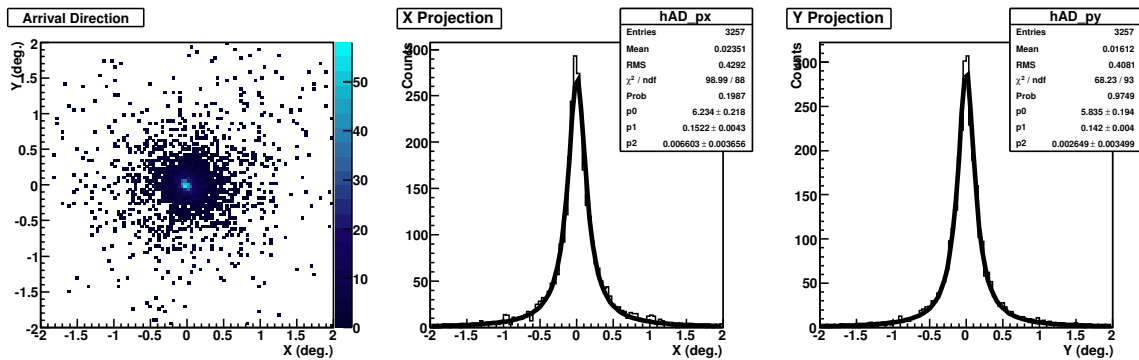

Figure 2. Distribution of reconstructed arrival directions obtained using the gamma-ray simulations. The middle and right histograms are X and Y projections of the left distribution, respectively.

4.2 Energy Resolution

At present, we conservatively use the mean image size of an event taken by the two telescopes as an energy estimator. The left of Figure 3 shows the distribution of mean sizes of simulated vertical gamma-ray events as a function of input energy. Here we also assume that the mean size is proportional to the gamma-ray primary energy on average and the line in the figure is a result of the proportional fit. The distribution of relative errors of estimated energies is shown in the right and the average energy resolution is estimated to be about 35% by fitting a Gaussian to the distribution. Again, the resolution is almost flat up to the zenith angle of $20°$.
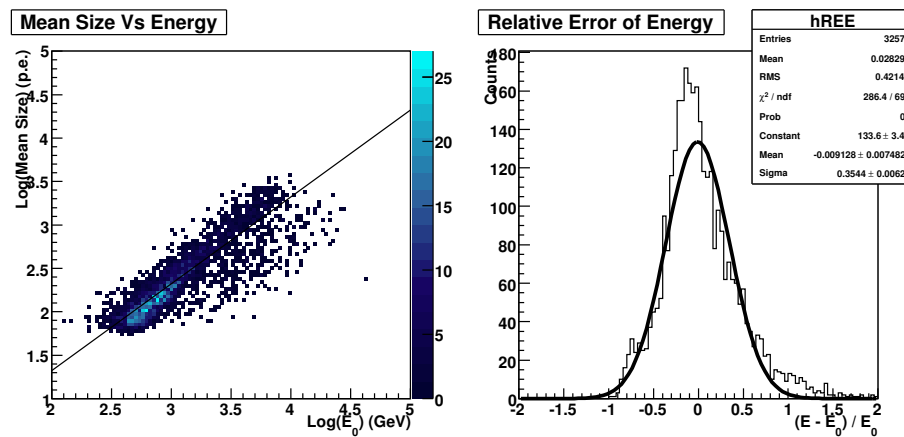
Figure 3. Distribution of mean sizes as a function of input energy (left). The energy estimation function is simply obtained as a proportional fit of the distribution and the distribution of relative errors of estimated energies is shown in the right.

5. Development in the Future

The energy resolution is expected to be improved by correcting the core distance dependence of Cherenkov light intensity. A preliminary analysis with this correction indicates that the energy resolution is improved by at least 10%. As a different point of view, the distance between a Cherenkov image and the source in the field of view is correlated with the core distance and effective use of the distance parameter is also under investigation as well as effective elimination of the camera edge effect.

6. Acknowledgements

References

[1] T.C. Weekes et al., ApJ, 342, 379 (1989).
[2] F.A. Aharonian et al., ApJ, 539, 317 (2000).
[3] T. Hara et al., NIM A 332, 300 (1993).
[4] K. Nishijima et al., 29th ICRC (Pune), in these proceedings (2005).
[5] A. Kawachi et al., Astropart. Phys., 14, 261 (2001).
[6] S. Kabuki et al., NIM A 500, 318 (2003).
[7] H. Kubo et al., 28th ICRC (Tsukuba), 5, 2863 (2003).
[8] GEANT - Detector Description and Simulation Tool, CERN Program Library Long Writeup W5013 (1993).
[9] T. Tanimori et al., 29th ICRC (Pune), in these proceedings (2005).